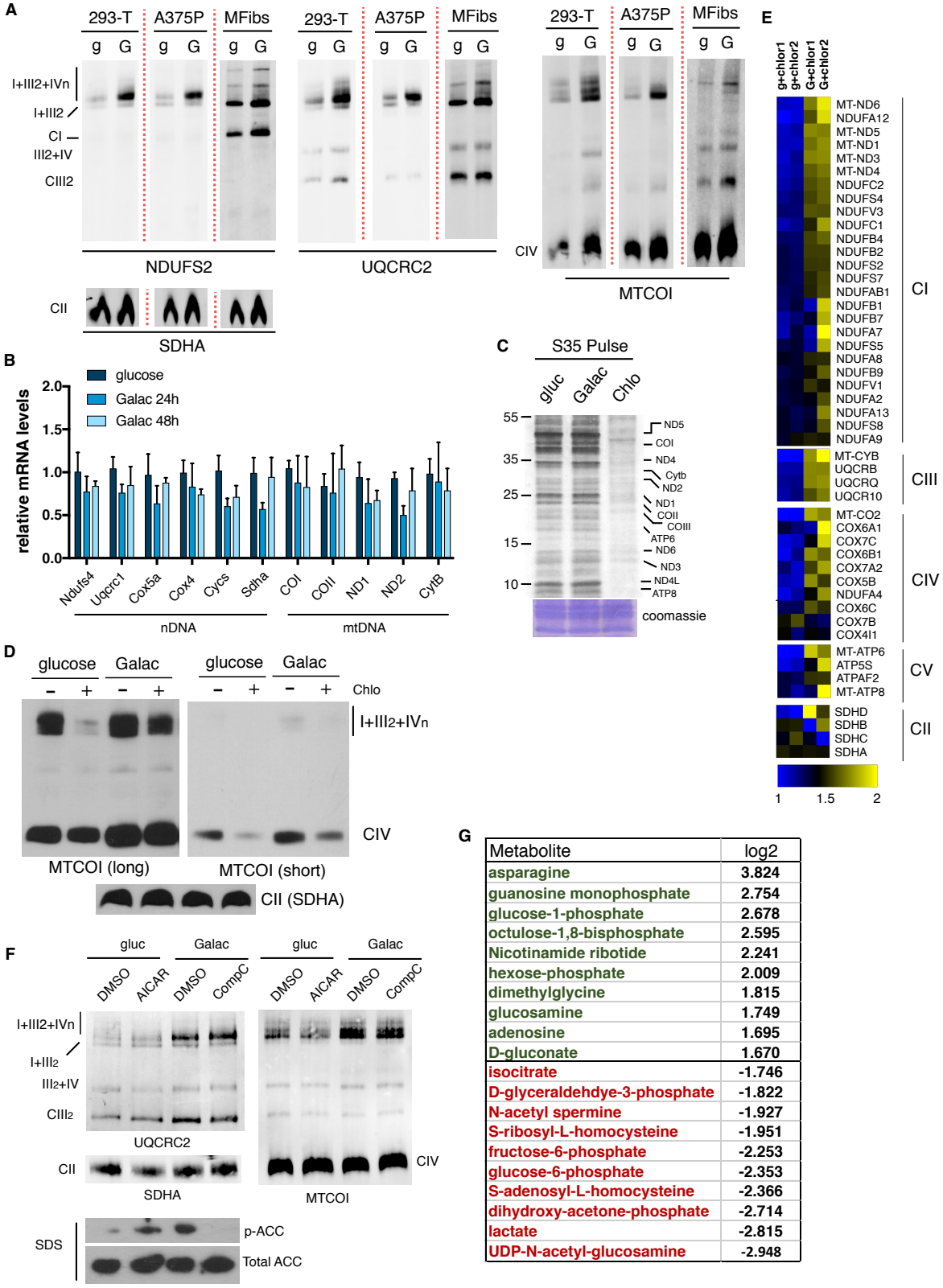


G

| Metabolite | log2 |
|---|---|
| asparagine | 3.824 |
| guanosine monophosphate | 2.754 |
| glucose-1-phosphate | 2.678 |
| octulose-1,8-bisphosphate | 2.595 |
| Nicotinamide ribotide | 2.241 |
| hexose-phosphate | 2.009 |
| dimethylglycine | 1.815 |
| glucosamine | 1.749 |
| adenosine | 1.695 |
| D-gluconate | 1.670 |
| isocitrate | -1.746 |
| D-glyceraldehdye-3-phosphate | -1.822 |
| N-acetyl spermine | -1.927 |
| S-ribosyl-L-homocysteine | -1.951 |
| fructose-6-phosphate | -2.253 |
| glucose-6-phosphate | -2.353 |
| S-adenosyl-L-homocysteine | -2.366 |
| dihydroxy-acetone-phosphate | -2.714 |
| lactate | -2.815 |
| UDP-N-acetyl-glucosamine | -2.948 |

**Figure S1. Glucose deprivation boost OXHPOS function. Related to Figure 1 & 2**

**A)** BNGE analysis in 293-T, A375P and mouse fibroblast cultured either in glucose or galactose for 48h. **(B)** qPCR analysis of mRNA levels of nuclear and mitochondrial encoded OXPHOS genes from U2OS cells cultured in either glucose or galactose. **(C)** $^{35}S$ pulse labeling experiment showing mitochondrial protein synthesis in cells cultured in glucose or galactose. Chloramphenicol treated cells in glucose conditions were used as a negative control. **(D)** Immunoblot of glucose or galactose cultured cells in the presence or absence of chloramphenicol for 24h. **(E)** Proteomic heat map showing elevated signal of OXPHOS components in cells cultured under galactose in the presence of chloramphenicol. **(F)** BNGE analysis from glucose or galactose-grown cells treated with the AMPK activator AICAR or inhibitor Compound C for 48h. Phosphorylation in ACC was used as indicator of AMPK activation **(G)** List of the top ten most up-regulated (green) and down-regulated (red) metabolites comparing glucose versus galactose-grown cells. SDHA was used as a loading control. Immunoblots shown are representative of >3 independent experiments. Data represent average ± SEM of three independent experiments. One-way ANOVA with Bonferroni post-test was applied. gluc, glucose. Galac, galactose. Chlo, Chloramphenicol.

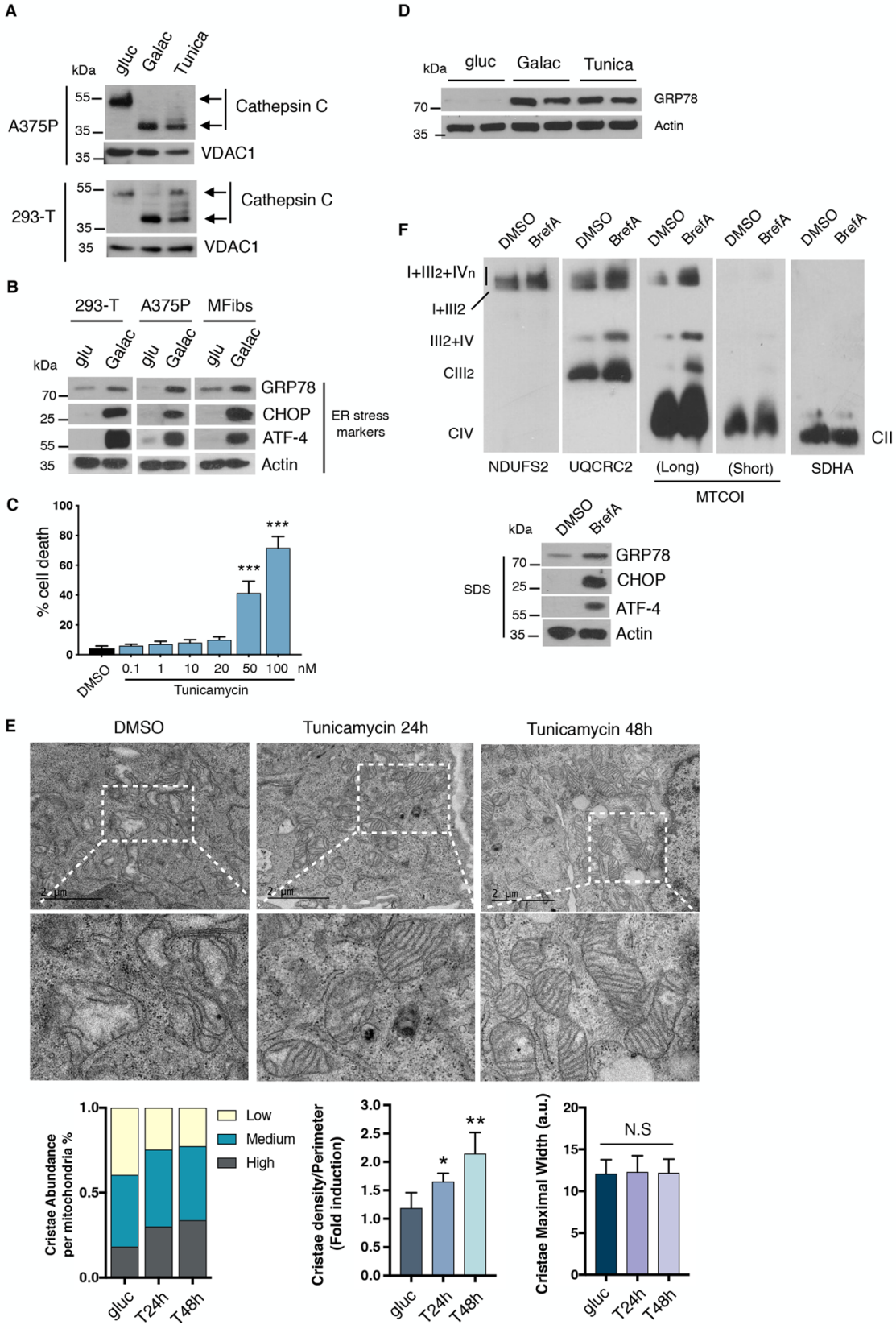
A
kDa
gluc
Galac
Tunica
A375P
55
35
Cathepsin C
35
VDAC1
293-T
55
35
Cathepsin C
35
VDAC1
B
293-T
A375P
MFibs
kDa
glu
Galac
glu
Galac
glu
Galac
70
GRP78
25
CHOP
55
ATF-4
35
Actin
ER stress markers
C
% cell death
100
80
60
40
20
0
***
***
DMSO
0.1
1
10
20
50
100
nM
Tunicamycin
D
kDa
gluc
Galac
Tunica
70
GRP78
35
Actin
F
DMSO
BrefA
DMSO
BrefA
DMSO
BrefA
DMSO
BrefA
DMSO
BrefA
I+III2+IVn
I+III2
III2+IV
CIII2
CIV
CII
NDUFS2
UQCRC2
(Long)
(Short)
SDHA
MTCOI
kDa
DMSO
BrefA
SDS
70
GRP78
25
CHOP
55
ATF-4
35
Actin
E
DMSO
Tunicamycin 24h
Tunicamycin 48h
2 µm
2 µm
2 µm
Cristae Abundance per mitochondria %
1.0
0.5
0.0
Low
Medium
High
gluc
T24h
T48h
Cristae density/Perimeter (Fold induction)
3.0
2.5
2.0
1.5
1.0
0.5
0.0
*
**
gluc
T24h
T48h
Cristae Maximal Width (a.u.)
20
15
10
5
0
N.S
gluc
T24h
T48h

**Figure S2. OXPHOS performance is induced by ER stress. Related to Figure 2**

**(A)** Immunoblots showing a shift in migration of Cathepsin C due to impaired ER protein glycosylation in the indicated cell lines. **(B)** Western blot analysis of ER stress markers: GRP78/BiP, CHOP and ATF4 in U2OS cells cultured in galactose at the indicated time points or in 293-T, A375P and mouse fibroblast at 48h. **(C)** U2OS cells were treated with increasing doses of tunicamycin for 48h and cell death was analyzed by Propidium Iodide Uptake and Flow Cytometry. **(D)** GRP78 levels in U2OS cells after tunicamycin or galactose treatment. **(E)** EM analysis of mitochondrial cristae morphology, abundance and density assayed in 24h and 48h tunicamycin treated cells. Data represent average ± SEM of three independent experiments. **(F)** SC levels and ER stress markers in Brefeldin A treated cells at 48h. Immunoblots shown are representative of >3 independent experiments. Tubulin, VDAC1, Actin or SDHA was used as a loading control. gluc, glucose. Galac, galactose. Tunica, tunicamycin. BrefA, Brefeldin A.

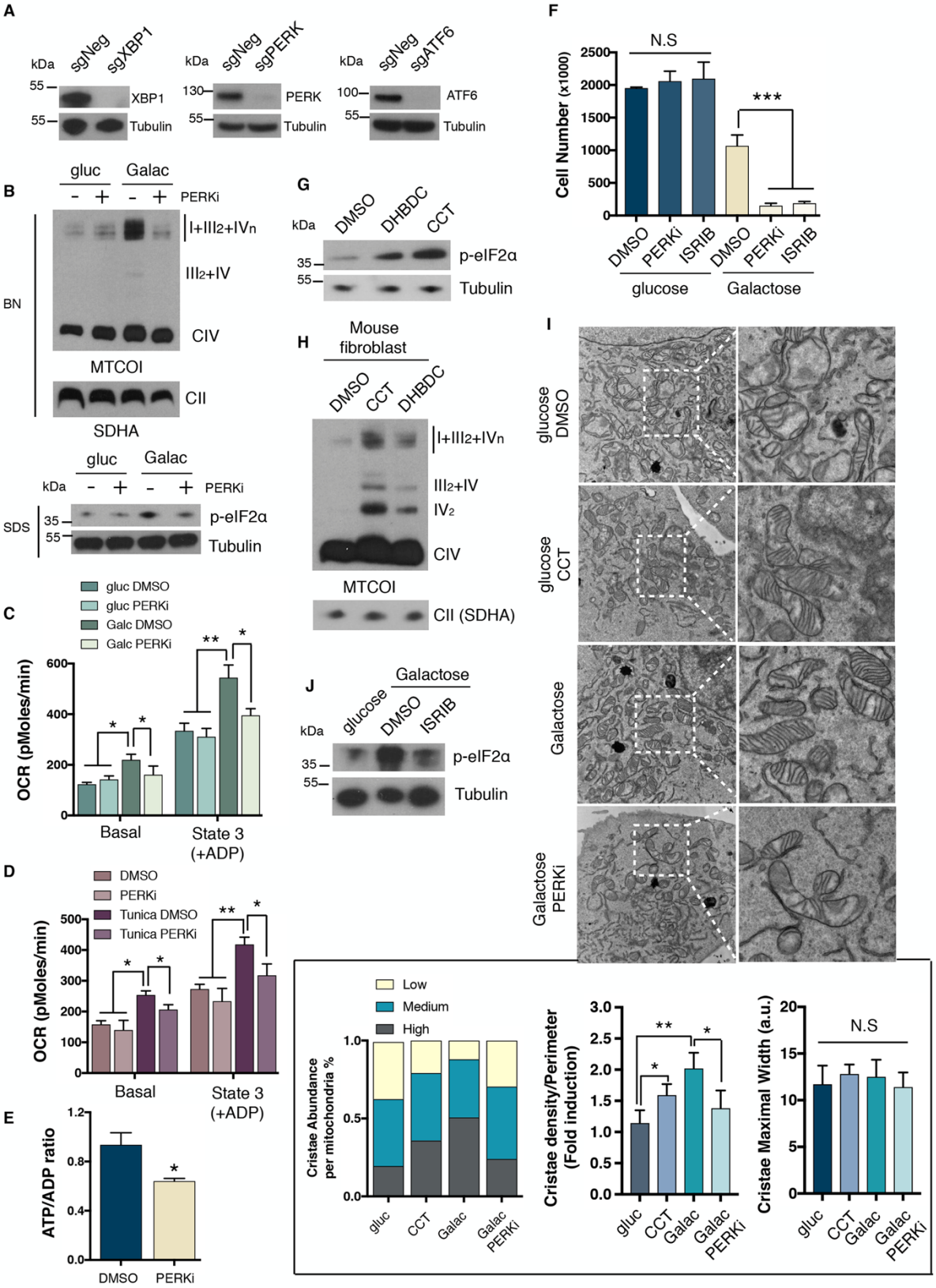
A
kDa
sgNeg
sgXBP1
55
XBP1
55
Tubulin
kDa
sgNeg
sgPERK
130
PERK
55
Tubulin
kDa
sgNeg
sgATF6
100
ATF6
55
Tubulin
B
gluc
Galac
- + - +
PERKi
BN
I+III2+IVn
III2+IV
CIV
MTCOI
CII
SDHA
gluc
Galac
kDa
- + - +
PERKi
SDS
35
55
p-eIF2α
Tubulin
C
gluc DMSO
gluc PERKi
Galc DMSO
Galc PERKi
OCR (pMoles/min)
600
400
200
0
Basal
State 3 (+ADP)
D
DMSO
PERKi
Tunica DMSO
Tunica PERKi
OCR (pMoles/min)
500
400
300
200
100
0
Basal
State 3 (+ADP)
E
ATP/ADP ratio
1.2
0.8
0.4
0.0
DMSO
PERKi
F
N.S
Cell Number (x1000)
2500
2000
1500
1000
500
***
DMSO
PERKi
ISRIB
DMSO
PERKi
ISRIB
glucose
Galactose
G
kDa
DMSO
DHBDC
CCT
35
55
p-eIF2α
Tubulin
H
Mouse fibroblast
DMSO
CCT
DHBDC
I+III2+IVn
III2+IV
IV2
CIV
MTCOI
CII (SDHA)
J
Galactose
glucose
DMSO
ISRIB
kDa
35
55
p-eIF2α
Tubulin
I
glucose DMSO
glucose CCT
Galactose
Galactose PERKi
Low
Medium
High
Cristae Abundance per mitochondria %
1.0
0.5
0.0
gluc
CCT
Galac
Galac PERKi
Cristae density/Perimeter (Fold induction)
3.0
2.5
2.0
1.5
1.0
0.5
0.0
gluc
CCT
Galac
Galac PERKi
Cristae Maximal Width (a.u.)
N.S
20
15
10
5
0
gluc
CCT
Galac
Galac PERKi

**Figure S3. PERK activation lead to increase ETC supercomplex and mitochondrial cristae. Related to Figure 3**

**(A)** Levels of XBP1, PERK and ATF6 after their depletion using CRISPR-CAS9 technology**.** **(B)** BNGE analysis in glucose or galactose-cultured cells after pharmacological inhibition of PERK. Note that PERK inhibition blocks galactose-induced eIF2α phosphorylation. **(C-D)**, Basal and state 3 respiration in isolated mitochondria with or without treatment with a PERK inhibitor. Mitochondrial respiration in cells cultured in galactose **(C)** or tunicamycin treatment for 24h **(D)**. **(E)** ATP/ADP ratios in galactose-cultured cells after PERK inhibition. **(F)** Cell proliferation and survival in U2OS cells treated with a PERK inhibitor or eIF2α inhibitor, ISRIB for 4 days. **(G)** eIF2α phosphorylation after PERK activation using DHBDC or CCT020312. **(H)** Immunodetection of the indicated proteins after BNGE of digitonin-solubilized mitochondria from mouse fibroblast after PERK activation. **(I)** Galactose-induced eIF2α phosphorylation blocked by ISRIB. (**I)** EM analysis of mitochondrial cristae morphology, abundance and density in U2OS cells challenged with PERK activator CCT020312, galactose and galactose plus PERK inhibitor. Data represent average ± SEM of three independent experiments. Tubulin or SDHA was used as a loading control. Experiments are the mean ± s.e.m., n>3. Asterisks denote *p<0.05 or **p<0.01. For two comparisons a two-tailed *t*-test was used, for multiple comparisons, one-way ANOVA with Bonferroni post-test was applied. gluc, glucose. Galac, galactose. Tunica, tunicamycin. PERKi, PERK inhibitor GSK2606414. CCT, CCT020312.

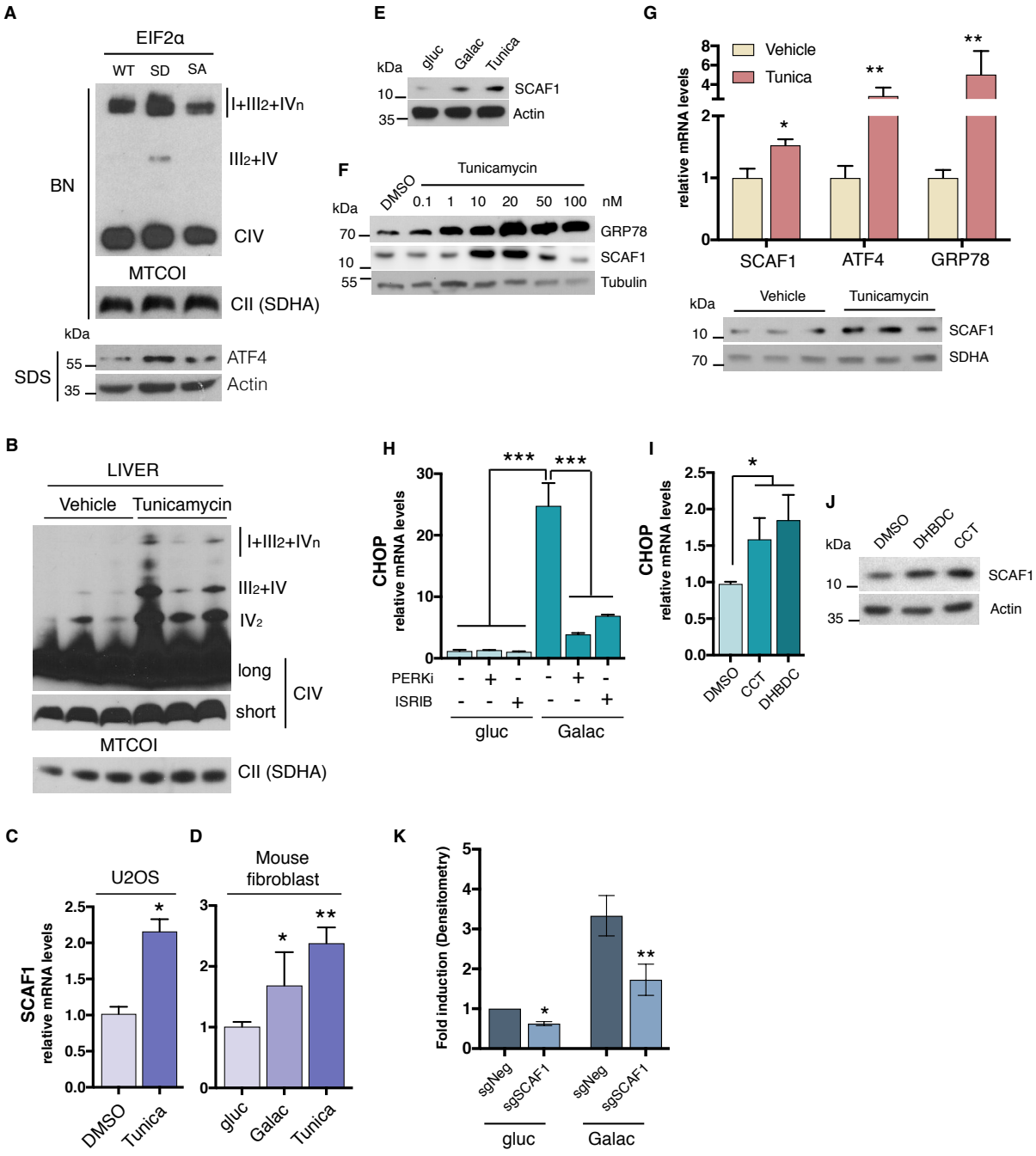
A
EIF2α
WT SD SA
I+III2+IVn
III2+IV
CIV
BN
MTCOI
CII (SDHA)
kDa
55
35
SDS
ATF4
Actin
B
LIVER
Vehicle Tunicamycin
I+III2+IVn
III2+IV
IV2
long
short
CIV
MTCOI
CII (SDHA)
C
U2OS
SCAF1 relative mRNA levels
DMSO Tunica
D
Mouse fibroblast
gluc Galac Tunica
E
kDa gluc Galac Tunica
10
35
SCAF1
Actin
F
Tunicamycin
kDa DMSO 0.1 1 10 20 50 100 nM
70
10
55
GRP78
SCAF1
Tubulin
G
Vehicle
Tunica
relative mRNA levels
SCAF1 ATF4 GRP78
kDa Vehicle Tunicamycin
10
70
SCAF1
SDHA
H
CHOP relative mRNA levels
PERKi
ISRIB
gluc Galac
I
CHOP relative mRNA levels
DMSO CCT DHBDC
J
kDa DMSO DHBDC CCT
10
35
SCAF1
Actin
K
Fold induction (Densitometry)
sgNeg sgSCAF1 sgNeg sgSCAF1
gluc Galac

**Figure S4. PERK/eIF2α/ATF4 axis transcriptionally regulate SCAF1 and promote Supercomplex formation. Related to Figure 3 & 4**

**(A)** SC levels of U2OS cells transfected with plasmids encoding wildtype (WT), phospho-mimetic (SD) or phospho-deficient (SA) eIF2α. **(B)** SC levels of isolated liver mitochondria from mice injected with tunicamycin (0.5 mg/kg) for 2 days. **(C)** SCAF1 mRNA levels in tunicamycin treated U2OS cells and **(D)** galactose-grown and tunicamycin treated mouse fibroblast. **(E)** Western blot analysis showing SCAF1 protein levels in cells cultured under galactose or tunicamycin conditions for 48h. **(F)** Levels of GRP78 and SCAF1 after treating U2OS cells with increasing doses of tunicamycin for 48h. **(G)** SCAF1 mRNA and protein levels in livers of vehicle and tunicamycin injected mice. **(**CHOP mRNA levels, as a readout of PERK activation, in **(H)** glucose and galactose-grown cells treated with PERKi (GSK2606414 500nM) or eIF2α phosphorylation inhibitors (ISRIB 200nM) or **(I)** PERK activators. **(J)** SCAF1 protein levels 72h after pharmacological PERK activation. **(K)** I+$II_2$+IVn bands from Fig 4D were quantified using ImageJ software and the fold induction from glucose to galactose in SCAF1 depleted cells is represented. Immunoblots shown are representative of >3 independent experiments. Actin or SDHA was used as a loading control. All other experiments are the mean ± s.e.m., n>3. Asterisks denote *p<0.05, **p<0.01 or ***p<0.001. For two comparisons a two-tailed *t*-test was used, for multiple comparisons, one-way ANOVA with Bonferroni post-test was applied. gluc, glucose. Galac, galactose. Tunica, tunicamycin. CCT, CCT020312.

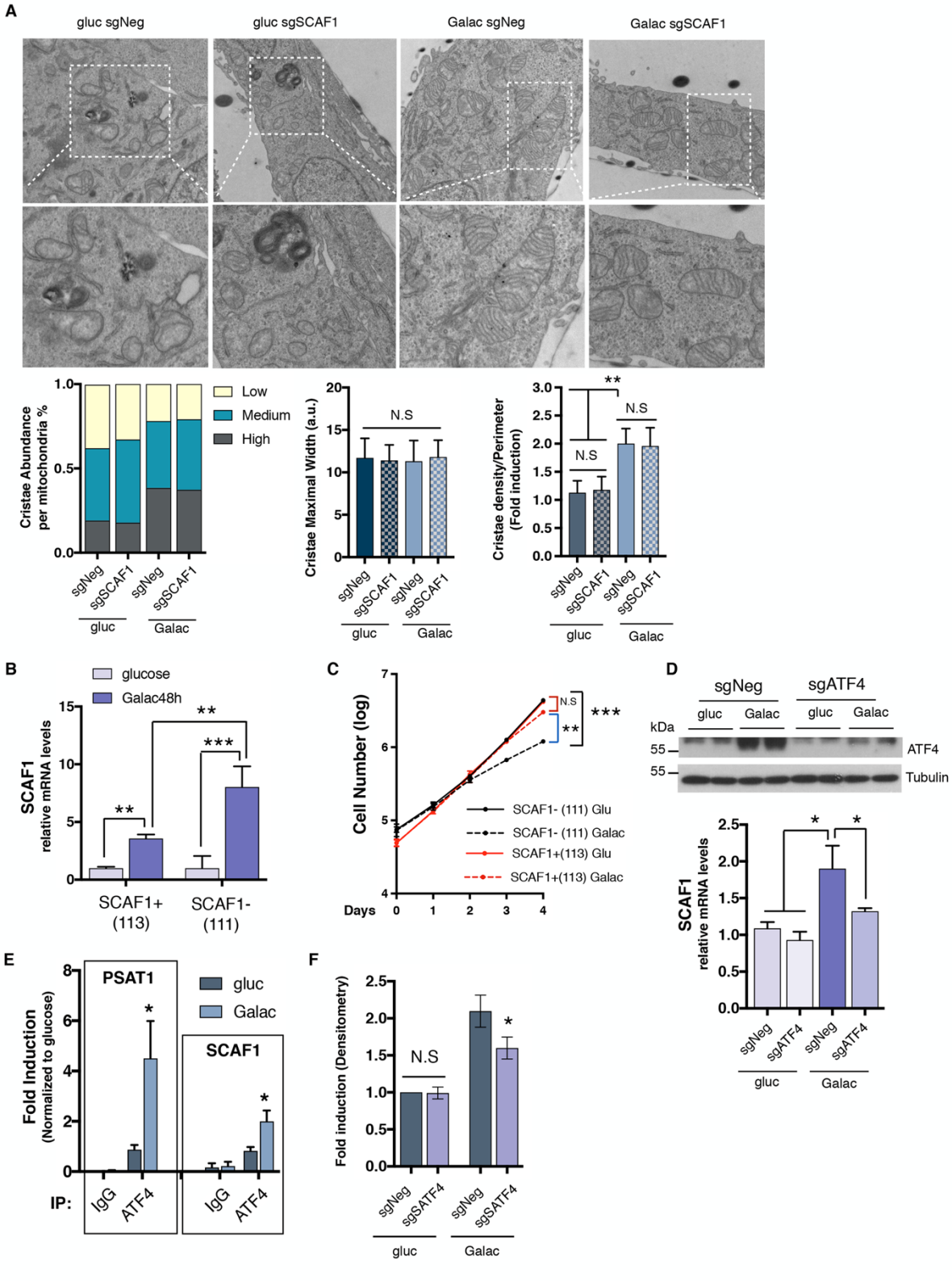
A
gluc sgNeg
gluc sgSCAF1
Galac sgNeg
Galac sgSCAF1
Cristae Abundance per mitochondria %
Low
Medium
High
sgNeg
sgSCAF1
gluc
Galac
Cristae Maximal Width (a.u.)
N.S
Cristae density/Perimeter (Fold induction)
**
B
glucose
Galac48h
SCAF1 relative mRNA levels
SCAF1+ (113)
SCAF1- (111)
C
Cell Number (log)
Days
SCAF1- (111) Glu
SCAF1- (111) Galac
SCAF1+(113) Glu
SCAF1+(113) Galac
***
D
sgNeg
sgATF4
kDa
ATF4
Tubulin
E
PSAT1
SCAF1
Fold Induction (Normalized to glucose)
IP:
IgG
ATF4
F
Fold induction (Densitometry)
sgSATF4

**Figure S5. SCAF1 is target of ATF4 and mediates adaptation to low glucose conditions. Related to Figure 4 & 5**

**A)** EM analysis of mitochondrial cristae morphology, abundance and density in glucose and galactose-grown U2OS cells with or without SCAF1. Data represent average ± SEM of three independent experiments. **(B)** SCAF1 mRNA levels and **(C)** cell growth curves of glucose versus galactose-grown mouse adult fibroblast carrying WT (113) or mutated (111) SCAF1**. (D)** Upper panel; CRISPR-mediated depletion of ATF4 in U2OS cells. Lower panel; SCAF1 mRNA levels in ATF4 depleted cells cultured in glucose or galactose. **(E)** ChIP assay showing ATF4 binding to SCAF1 promoter. The *bona fide* ATF4 target gene PSAT1 was used as a positive control. **(F)** I+$III_2$+IVn bands were quantified from figure 4H using ImageJ software and fold induction of glucose versus galactose ATF4 depletion is represented. Actin or Tubulin was used as a loading control. Immunoblots shown are representative of >3 independent experiments. Asterisks denote, *p<0.05, **p<0.01 or ***p<0.001. For two comparisons a two-tailed *t*-test was used, for multiple comparisons, one-way ANOVA with Bonferroni post-test was applied. gluc, glucose. Galac, galactose. PERKi, PERK inhibitor GSK2606414.

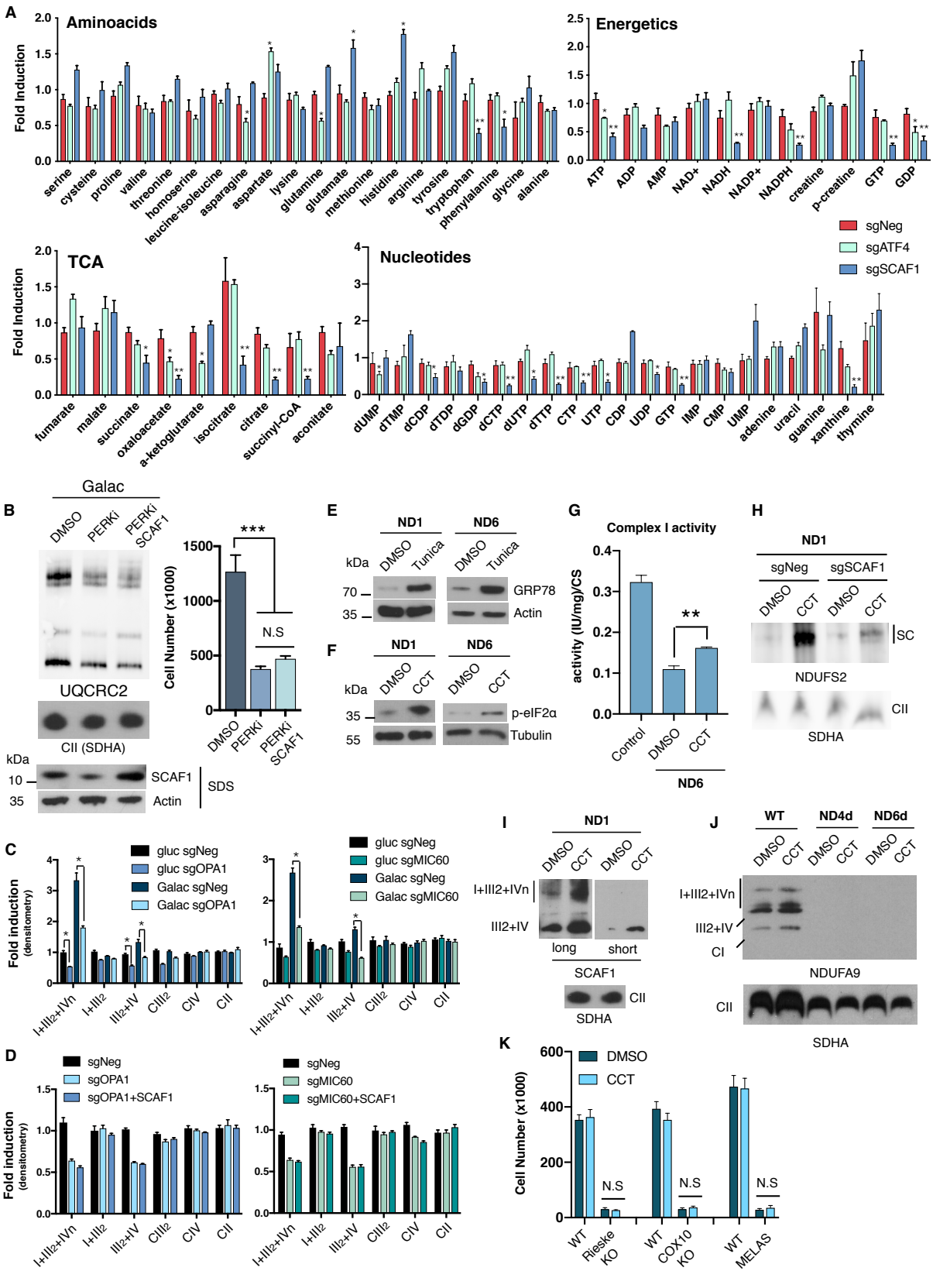
A
Aminoacids
Fold Induction
serine
cysteine
proline
valine
threonine
homoserine
leucine-isoleucine
asparagine
aspartate
lysine
glutamine
glutamate
methionine
histidine
arginine
tyrosine
tryptophan
phenylalanine
glycine
alanine
Energetics
ATP
ADP
AMP
NAD+
NADH
NADP+
NADPH
creatine
p-creatine
GTP
GDP
TCA
fumarate
malate
succinate
oxaloacetate
a-ketoglutarate
isocitrate
citrate
succinyl-CoA
aconitate
Nucleotides
dUMP
dTMP
dCDP
dTDP
dGDP
dCTP
dUTP
dTTP
CTP
UTP
CDP
UDP
GTP
IMP
CMP
UMP
adenine
uracil
guanine
xanthine
thymine
sgNeg
sgATF4
sgSCAF1
B
Galac
DMSO
PERKi
PERKi SCAF1
UQCRC2
CII (SDHA)
kDa
SCAF1
Actin
SDS
Cell Number (x1000)
***
N.S
C
gluc sgNeg
gluc sgOPA1
Galac sgNeg
Galac sgOPA1
gluc sgMIC60
Galac sgMIC60
Fold induction
(densitometry)
I+III2+IVn
I+III2
III2+IV
CIII2
CIV
CII
D
sgNeg
sgOPA1
sgOPA1+SCAF1
sgMIC60
sgMIC60+SCAF1
E
ND1
ND6
Tunica
GRP78
Actin
F
CCT
p-eIF2α
Tubulin
G
Complex I activity
activity (IU/mg)/CS
**
Control
H
sgNeg
sgSCAF1
SC
NDUFS2
CII
SDHA
I
long
short
J
WT
ND4d
ND6d
CI
NDUFA9
K
Cell Number (x1000)
Rieske KO
COX10 KO
MELAS

**Figure S6. PERK activation rescues Complex I levels and bioenergetics in mitochondrial mutant cells. Related to Figure 5 & 6**

**(A)** U2OS sgNeg, sgATF4 and sgSCAF1 cells were culture in galactose media for 48h and intracellular metabolites were extracted and analyzed via LC-MS. Data are means of triplicate wells. **(B)** SC levels (left) and cell proliferation (right) under galactose, in PERK inhibited cells (for 4 days) with or without ectopic overexpression of SCAF1. Bands from figure 5A **(C)** or figure 5B **(D)** were quantified using ImageJ software and represented as fold induction. **(E)** GRP78 levels were used as a marker of ER stress after tunicamycin treatment **(F)** eIF2α phosphorylation levels after CCT020312 treatment. **(G)** Complex I mitochondrial enzymatic activity in ND6 cells treated with either DMSO or CCT020312 compared to control cybrids. **(H)** Complex I levels in SC of ND1 sgNeg and sgSCAF1 cells treated for 72h with CCT020312. **(I)** ND1 cybrid SCAF1 protein levels incorporated into SC formation in the presence or absence of CCT020312. **(J)** SC levels in WT, ND4d, or ND6d mouse fibroblast treated with DMSO or CCT020312 for 72h. **(K)** PERK activation did not rescue galactose-induced cell death in tRNA-mutated cybrids (MELAS) or, CIII (Reiske) and CIV (Cox10) Knock-out fibroblasts. Immunoblots shown are representative of >3 independent experiments. Actin, SDHA or Tubulin was used as a loading control. All other experiments are the mean ± s.e.m., n>3. Asterisks denote **p<0.01. For two comparisons a two-tailed *t*-test was used, for multiple comparisons, one-way ANOVA with Bonferroni post-test was applied. gluc, glucose. Galac, galactose. Tunica, tunicamycin. CCT, CCT020312.